ISSN: 2277-9655
Impact Factor: 3.785

IJESRT

INTERNATIONAL JOURNAL OF ENGINEERING SCIENCES & RESEARCH TECHNOLOGY

EVALUATION OF MACHINING INDUCED RESIDUAL STRESSES IN 2014 A T6 ALUMINUM ALLOY USING INDENTATION METHOD AND ITS CO-RELATION TO DISTORTION DUE TO TOOL PATH LAYOUTS

Mr.S.V.Prasad*, Dr.P.LaxmiNarayana, Dr.P.Ravinder Reddy
* Senior Manager,Designs,HAL,Hyd,India
Professor,Dept of ME,Osmania University,Hyd,India
Professor&Head, Dept. of ME., CBIT, Hyd ,India

DOI: 10.5281/zenodo.51912

ABSTRACT

In this work, effect of different tool path layouts on machining induced residual stresses and in turn on distortion in aluminum alloy 2014 A T6 were studied by calculating residual stresses using indentation method. Results showed that tool path layout effect the residual stress distribution and lead to distortion. Machining induced stresses by using pocket out machining were minimum leading to minimum distortion.

KEYWORDS: Machining, Distortion, Residual stress, Indentation Method, Aluminum Alloy.

INTRODUCTION

Stresses and part distortion have a major cost impact in many machining applications since they can affect scrap rates and processing times. For example, in Avionic monolithic components they may produce distortions which hamper assembly operations. Stresses in machined parts result from two sources. Prior to machining, bulk stresses from primary processes such as rolling or forging may be present in the work piece and the stresses induced by the machining process, which result from differential plastic deformation and surface temperature gradients [1]. Selection and application of tool path strategies and tool orientations in the process of milling is an important issue in machining of monolithic thin walled thin floored Avionics components.

Distortion during machining can result in high scrap rates and increased manufacturing costs. Distortion results from either the introduction or elimination of stresses during manufacture. Stresses which are induced in the surface by machining can generally be measured and controlled. Distortion caused by re-equilibration after removal of stressed material during machining is more difficult to avoid, and is the primary cause of scrap in precision components.
During machining, the distortion of a part depends upon the geometry, order of removal, and stress state in the material removed. If the change of shape which occurs is not accommodated, the part maybe scrapped during machining. One of the important parameter in controlling the machining induced stress is the tool path layout adopted during machining. The stress distributions typically seen in machining of components in each tool path layout for 2014 T6aluminum alloy are presented in the following experiment.

RELATED WORK

Different experimental techniques have been developed and greatly improved in order to determine with high accuracy the residual stresses generated in the processing of engineering materials [2], [3], [4].In the case of machining, two approaches are widely used: X-ray diffraction technique[5],[6] ,[7] and the hole-drilling method [8]. However, in recent years different techniques based on instrumented indentation have been used in order to study different issues of residual stresses in machining. The method of indent pairs was developed by Wyatt and Berry in order to perform different studies of residual stresses in high-speed milled components .The method of indent pairs consists in

determining the change in indent spacing, which is produced when the specimen is subjected to a distension procedure [9].

An experimental study on representative monolithic work piece was made to show the influence of spiral in and spiral out cutter path strategies and tooth loading on part distortion. The study suggested two different machining cutter path strategies has shown less influence on part distortion for a given offset [10]. The prediction of cutting forces and the distribution law of residual stresses are studied using pocket in and pocket out milling strategies and concluded that the more fluctuant distribution of the residual stresses at the final path than the first path is resulted from the gradual application of dynamic milling forces on the aeronautical monolithic component [11].

In other machining processes, Fuh developed an empirical model to predict the residual stresses produced by milling of 2014-T6 aluminum. The mathematical model integrated cutting environment like cutting speed, feed, and cutting depth as well as tool geometry characteristics known as flank wear and nose radius [12].
A significant amount of work has been done on impact of tool parameters and process parameters on part distortion. An attempt in understanding the influence of tool path layouts on part distortion in machining is made in this paper.

EXPERIMENTAL PROCEDURE

3.1 Materials and equipment.

The work piece material used is aluminum alloy 2014A T6 rolled plate. This material is used in manufacture of avionics components, as it has high strength to weight ratio, thermal and electrical conductivity when compared to other grades of aluminum alloys. The chemical and mechanical properties of the material under study are mentioned in Table1 and Table2 respectively [13].

Table 1: Chemical composition of aluminum alloy 2014A T6

PROPERTY	VALUE
Copper	3.8 to 4.8
Magnesium	0.2 to 0.8
Silicon	0.6 to 0.9
Iron	0.7 max
Manganese	0.2 to 1.2
Aluminium	Reminder

Table2: Mechanical Properties of 2014A T6

Property	Value
Yield strength	380 Mpa
Tensile strength	405 Mpa
Hardness Rockwell B	82
Density	2.80 g/cc
Poisson's Ratio	0.2

The work pieces are held in the shop made vacuum fixture connected to the WITTIE vacuum pump (Figure 1)and machining is done on Hardinge Bridgeport (VMC 600P3) CNC machining centre (Figure 2) with constant tool and cutting parameters in various tool path layoutsas shown in Table3 and Figure 3 respectively.

ISSN: 2277-9655
Impact Factor: 3.785

Figure 1. WITTIE vacuum Pump

Figure 2. Hardinge Bridgeport (VMC 600P3)

Table 3. Tool geometry and cutting parameters

TOOL MATERIAL AND DIAMETER	HELIX ANGLE	No.OF FLUTES	R.P.M	FEED PER TOOTH	DEPTH OF CUT	WIDTH OF CUT
Solid Carbide End mill of 20mm diameter	30 deg	2	5000	0.1	3mm	6mm

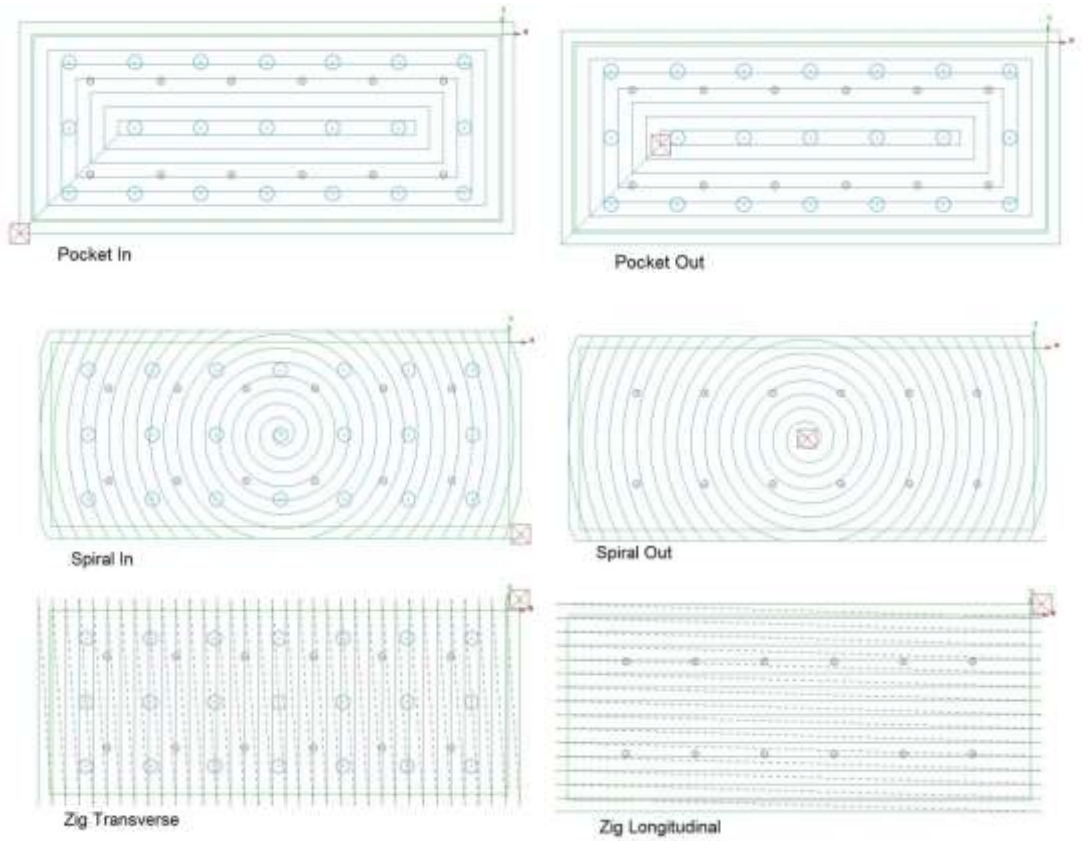

ISSN: 2277-9655
Impact Factor: 3.785

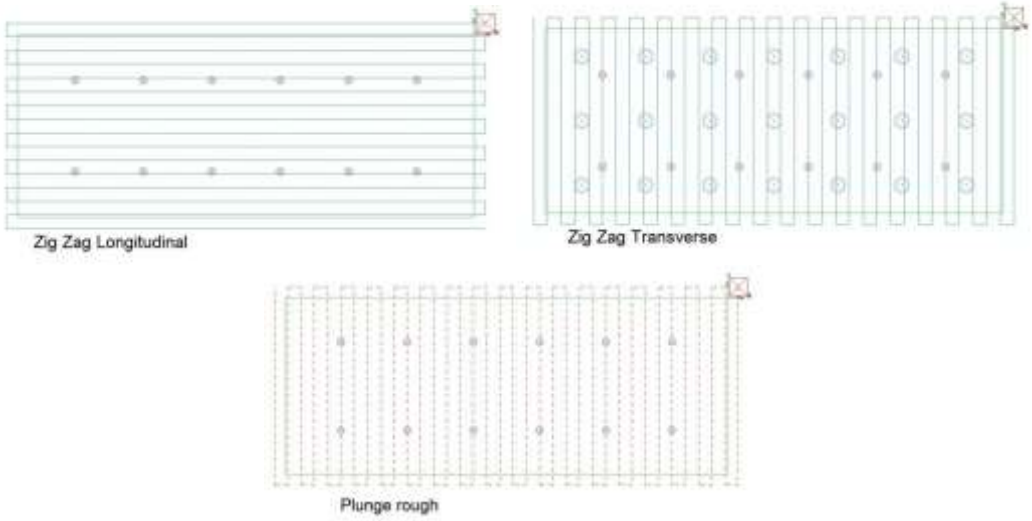

---------- Rapid movement
_____Feed movement
Figure 3: Tool path layouts

The indents on the work piece are made with the indenter having an included angle of 120º. The measurements are accurately taken with optical measuring equipment Baty Vision Systems - Venture VI-3030 CNC (Figure 4), which has a resolution of 0.5 micron and 40 X magnification.

Figure 4: Baty Vision System-Venture VI-3030 CNC

3.2 Experimental work

The dimensions of the samples taken are 5mm x 80mm x 200mm.Prior to machining, the samples are stress relieved to a temperature of 200ºC for 2 hrs. so as to ensure that the bulk residual stresses are made minimum. This will reduce the error on evaluation of distortion in the material due to machining induced stresses.

The material is machined from 5mm thick to 2mm thick in different tool path layouts. Without removing the work piece from the fixture the indents are made at a pitch of 30mm along X axis (lengthier side) and at a pitch of 40mm along Y axis (shorter side) as shown in Figure5.

ISSN: 2277-9655
Impact Factor: 3.785

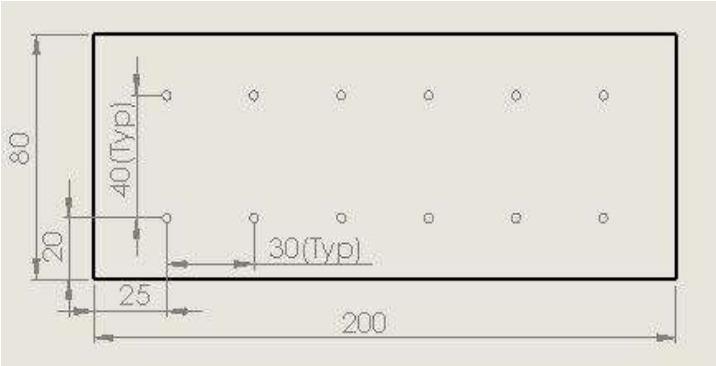

Figure 5: Work piece and indents dimensions

The flow diagram of the overall procedure is shown in Figure 6.

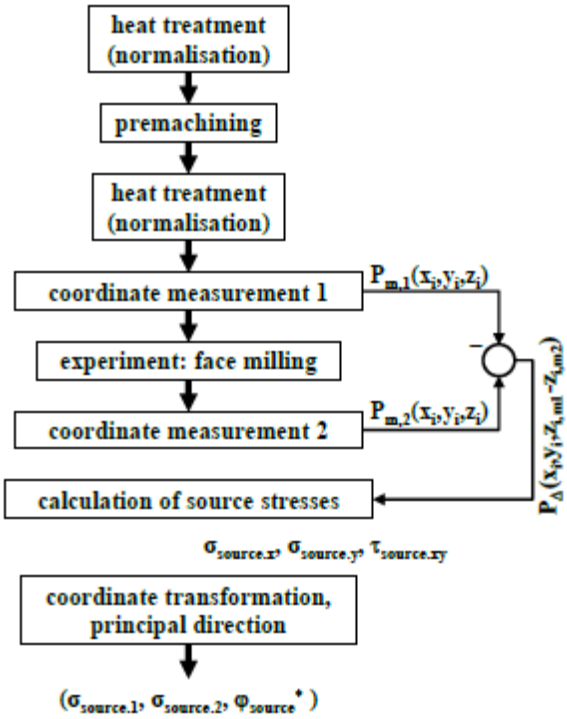

Figure 6: Flow diagram of the overall procedure

3.3 Calculation of strain and stress

The collinear distance between the coordinates of the indents before and after re-equilibration of machining induced stresses are accurately measured. For each of the intended indent it is possible to determine normal components of the residual strain in three directions (ε_x, ε_y and ε_d). Two of these (corresponding to ε_x and ε_y) are perpendicular and in turn parallel to the sides of the rectangle defined by the indents, as shown in Figure7, [14] and [15].

ISSN: 2277-9655
Impact Factor: 3.785

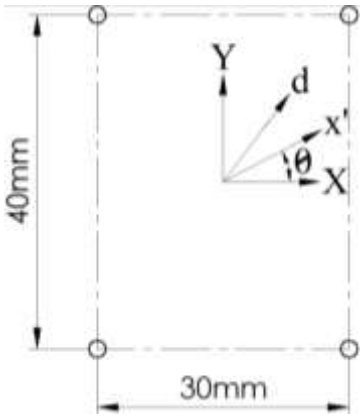

Figure 7: Directions corresponding to ε_x, ε_y and ε_d

The remaining direction (associated to εd) corresponds to the bisector of the other directions. Such normal components of the residual strain can be expressed as shown in equation 1

$$\varepsilon x=\frac{lx}{lx'}-1 \qquad \varepsilon y=\frac{ly}{lx'}-1 \qquad \varepsilon d=\frac{ld}{ld'}-1 \tag{1}$$

where lx andlx' are the mean values of the horizontal sides of the rectangle defined by the indents and ly and ly'are the mean values of the vertical sides, in both cases before and after re-equilibration of stresses(before and after removing from the vacuum fixture).ld and ld' correspond to the positive slope diagonal of the aforesaid rectangle, also before and after removing the work piece from the vacuum fixture. Then from the normal components it is possible to obtain the tangential component (ϒxy) from equation 2 [16]

$$\Upsilon xy=2.\varepsilon d-\varepsilon x-\varepsilon y \tag{2}$$

As the heat treatment is done below the recrystallization temperature of the material, the dimensional change of the evaluated surface will be caused by the elastic relaxation of the lattice [17], [18]. Therefore if the evaluated surface is considered to be under plane stress conditions the orthogonal components of the residual stress can be expressed for isotropic, linear elastic materials as in equations (3),(4) & (5)

$$\sigma x = k1.\varepsilon x + k2.\varepsilon y \tag{3}$$

$$\sigma y = k1.\varepsilon y + k2.\varepsilon x \tag{4}$$

Where $k1=E/(1-\nu 2)$, $k2=\nu.k1$. (5)

E is the longitudinal elastic modulus and ν is the poisson's ratio.

Assuming that the generated surface is under a plane stress state and the evaluated material is linearly elastic, homogenous and isotropic, the residual stress components from (6) and (7)

$$\sigma x' = \frac{\sigma x+\sigma y}{2}+\frac{\sigma x-\sigma y}{2}.\cos 2\theta+\tau xy.\sin 2\theta \tag{6}$$

$$\tau x'y'=\frac{\sigma x-\sigma y}{2}.\sin 2\theta+\tau xy.\cos 2\theta \ . \tag{7}$$

The calculated values of stress in X, Stress in Y and τxy at centre of the rectangular areas defined by the indents in each of the nine tool path strategies are detailed in Table 4.The stress distribution profiles along X-axis and along Y-axis in each of the tool path strategies are shown in Figure 9.

ISSN: 2277-9655
Impact Factor: 3.785

Table 4: Stress values in different toolpath layouts

	POCKET IN				POCKET OUT				ZIG LOGITUDINAL		
S.No	STRESS IN X (MPa)	STRESS IN Y(MPa)	TXY (MPa)	S.No	STRESS IN X (MPa)	STRESS IN Y (MPa)	TXY (MPa)	S.No	STRESS IN X (MPa)	STRESS IN Y (MPa)	TXY (MPa)
1	-49.18996	-46.22969	-0.00081	1	41.83632	20.17217	-0.00001	1	31.68902	0.45563	-0.00157
2	3.55582	-37.00029	-0.00041	2	-8.86321	2.53180	-0.00101	2	5.73939	13.71780	0.00035
3	-8.19666	-76.28977	-0.00153	3	39.66263	54.03357	-0.00073	3	10.21981	108.10121	-0.00096
4	63.94067	-37.96097	-0.00027	4	27.09930	41.69501	0.00030	4	26.59894	91.62501	0.00019
5	-56.43494	-16.80473	0.00047	5	51.28460	45.12547	-0.00017	5	13.91812	12.77828	0.00034

	ZIG TRANSVERSE				ZIG ZAG LONGITUDINAL				ZIG ZAG TRANSVERSE		
S.No	STRESS IN X (MPa)	STRESS IN Y (MPa)	TXY (MPa)	S.No	STRESS IN X (MPa)	STRESS IN Y (MPa)	TXY (MPa)	S.No	STRESS IN X (MPa)	STRESS IN Y (MPa)	TXY (MPa)
1	17.82587	65.03998	0.00040	1	67.56226	68.70325	0.00230	1	48.88394	48.88394	0.00052
2	13.81456	41.86230	-0.00004	2	94.08082	12.86372	-0.00030	2	-64.87652	-35.04732	0.00053
3	-26.25489	12.25753	0.00016	3	-24.47197	-11.71307	-0.00085	3	-2.81820	-59.99139	-0.00112
4	28.58424	9.43280	-0.00055	4	5.95348	51.10407	0.00104	4	22.71873	-52.47210	-0.00003
5	43.22816	13.35593	-0.00010	5	23.60572	67.85820	-0.00041	5	-46.51086	-34.44045	0.00069

	SPIRAL IN				SPIRAL OUT				PLUNGE ROUGH		
S.No	STRESS IN X (MPa)	STRESS IN Y (MPa)	TXY (MPa)	S.No	STRESS IN X (MPa)	STRESS IN Y (MPa)	TXY (MPa)	S.No	STRESS IN X (MPa)	STRESS IN Y (MPa)	TXY (MPa)
1	-30.34479	14.54763	0.00017	1	-10.77226	-32.64321	0.00117	1	9.52189	-74.07261	-0.00162
2	48.63203	26.05307	-0.00144	2	-34.40555	-82.21599	-0.00059	2	-94.45326	-128.34273	-0.00128
3	33.12917	-17.24708	0.00010	3	-35.22902	-47.98240	0.00019	3	20.56947	-99.45357	-0.00115
4	-20.32427	-28.52546	0.00040	4	49.61695	-40.87195	-0.00029	4	14.35272	-85.18046	-0.00174
5	-6.47931	2.40899	0.00071	5	-133.34232	-88.53507	0.00144	5	-98.78711	-148.81380	-0.00071

POCKET IN TOOL PATH LAYOUT

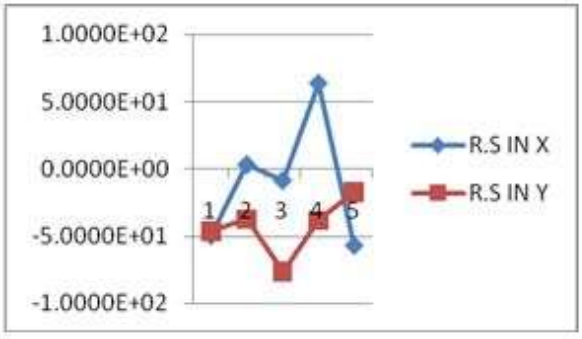

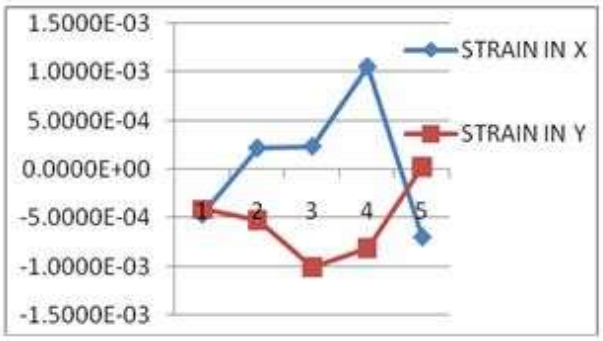

ISSN: 2277-9655
Impact Factor: 3.785

POCKET OUT TOOL PATH LAYOUT

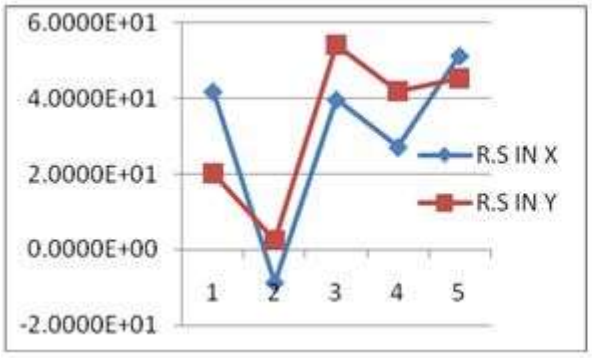

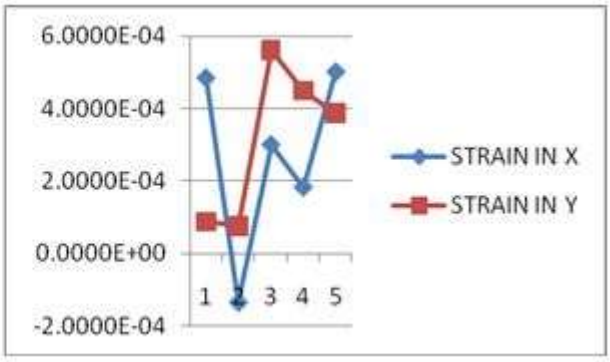

ZIG LONGITUDNAL TOOL PATH LAYOUT

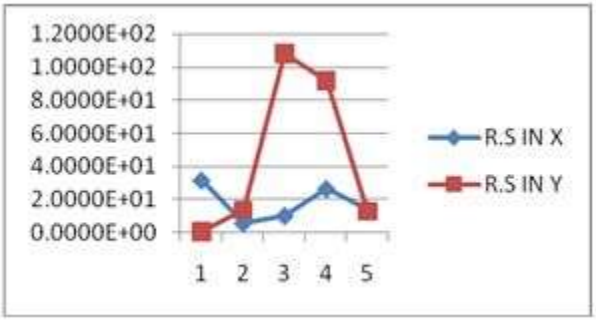

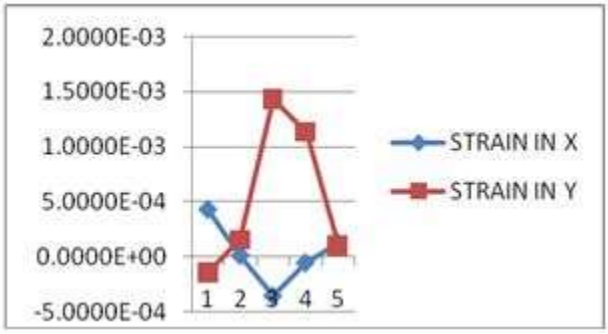

ZIG TRANSVERSE TOOL PATH LAYOUT

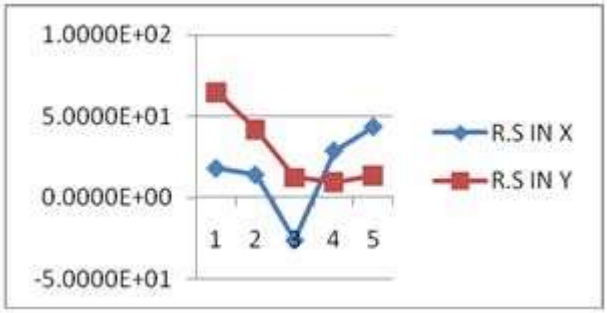

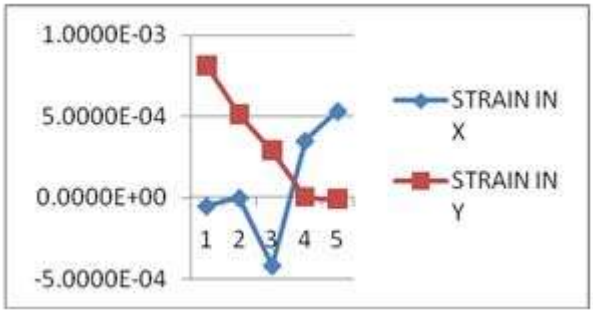

ZIG ZAG LONGITUDNAL TOOL PATH LAYOUT

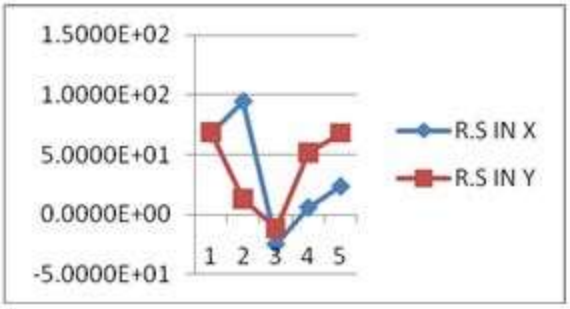

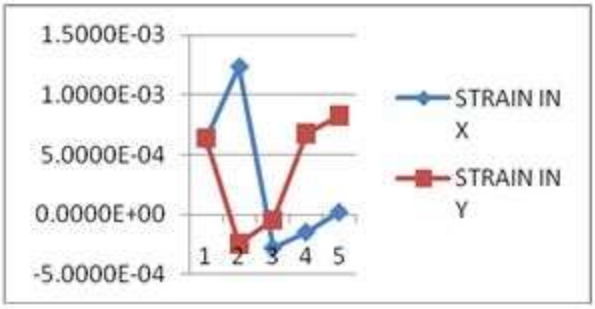

ISSN: 2277-9655
Impact Factor: 3.785

ZIG ZAGTRANSVERSE TOOL PATH LAYOUT

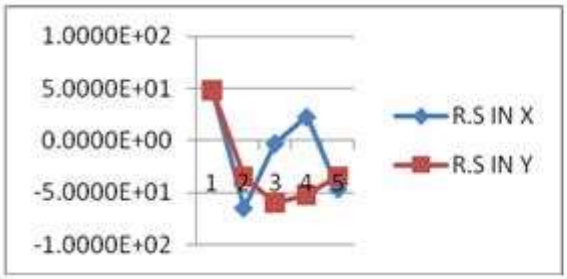

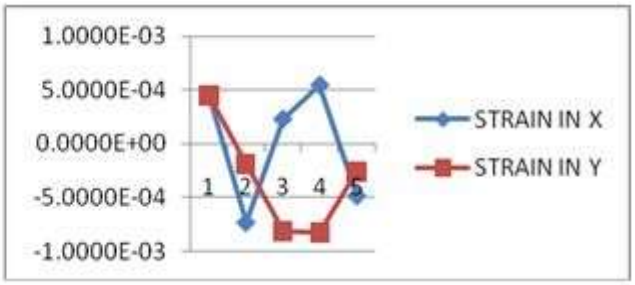

SPIRAL IN TOOL PATH LAYOUT

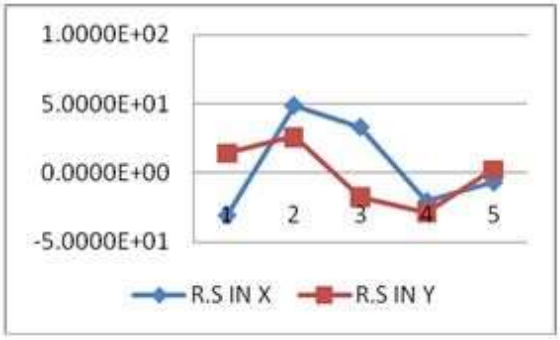

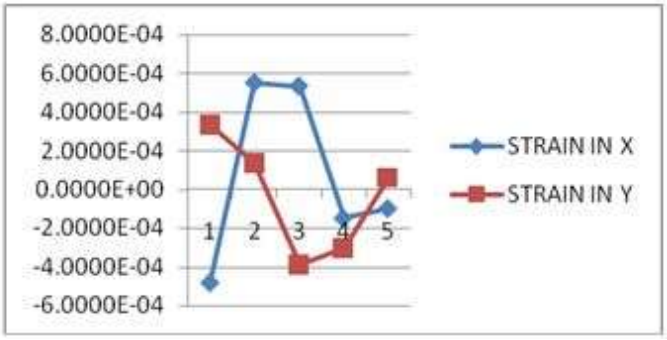

SPIRAL OUT TOOL PATH LAYOUT

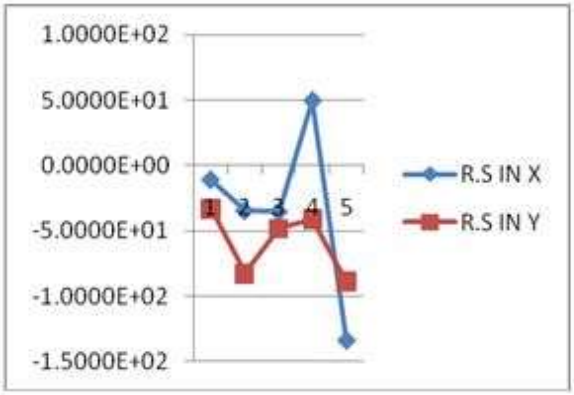

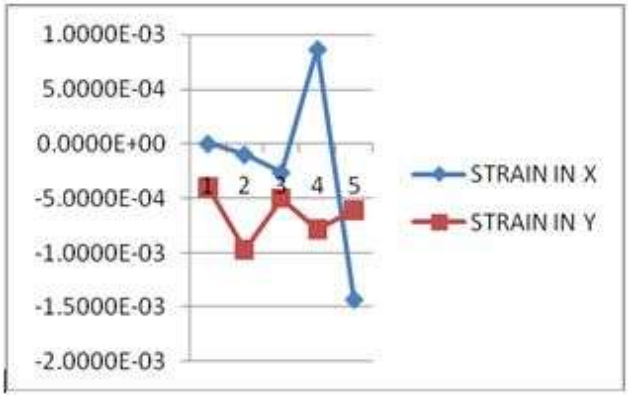

PLUNGE ROUGH TOOL PATH LAYOUT

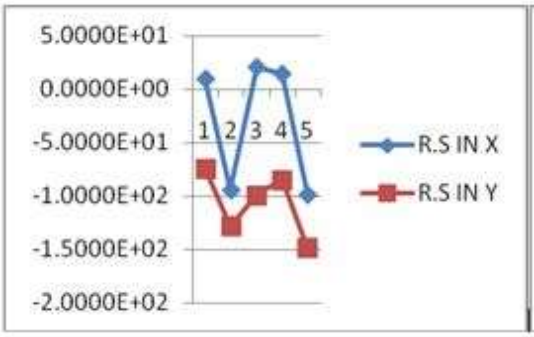

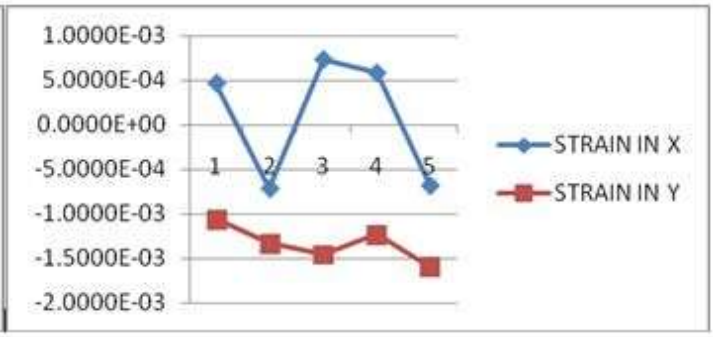

ISSN: 2277-9655
Impact Factor: 3.785

For measuring the geometry of the work piece before and after machining, a grid of 15 x 7 points with a pitch of 12 x 10 is marked on the backside of each work piece as shown in Figure 8. Each coordinate measurement provided 105 coordinate triplets describing the work piece surface as a point cloud. The geometry is measured opposite the surface machined during the experiments. In this way the effect of the machining induced source stresses could be isolated from the thermal effects. The 3D geometric profile using the point cloud data is modeled using "SOLIDWORKS 2013" CAD package. The machining is done using "CAMWORKS 2013" CAM package. The modeled distortion profiles from the measured point cloud after machining is shown in Figure 10.The value in z axis is magnified 50 times to significantly show the distortion profile in each of the tool path layouts. Hence the images are indicative in nature.

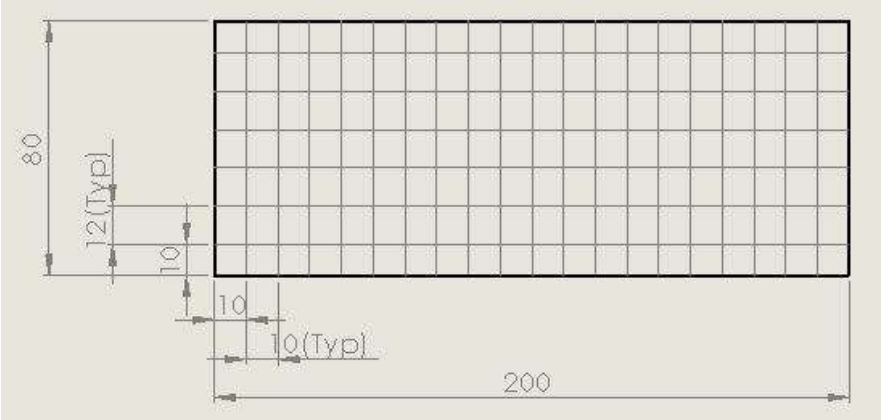

Figure 8: Grid on the work piece for measurement

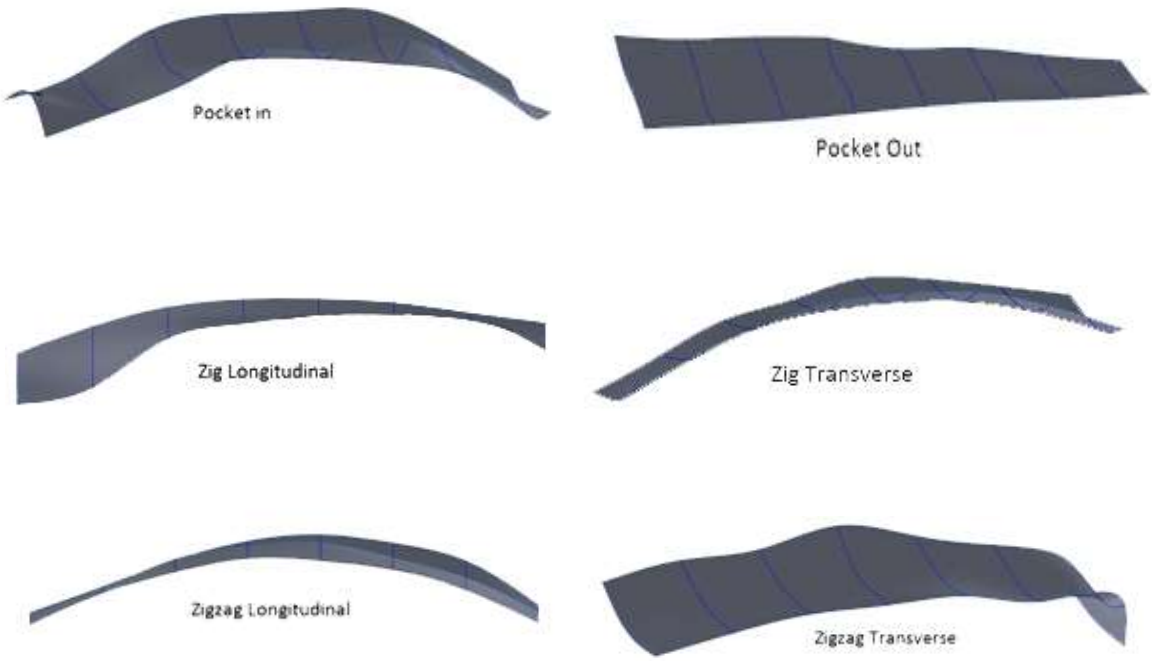

ISSN: 2277-9655
Impact Factor: 3.785

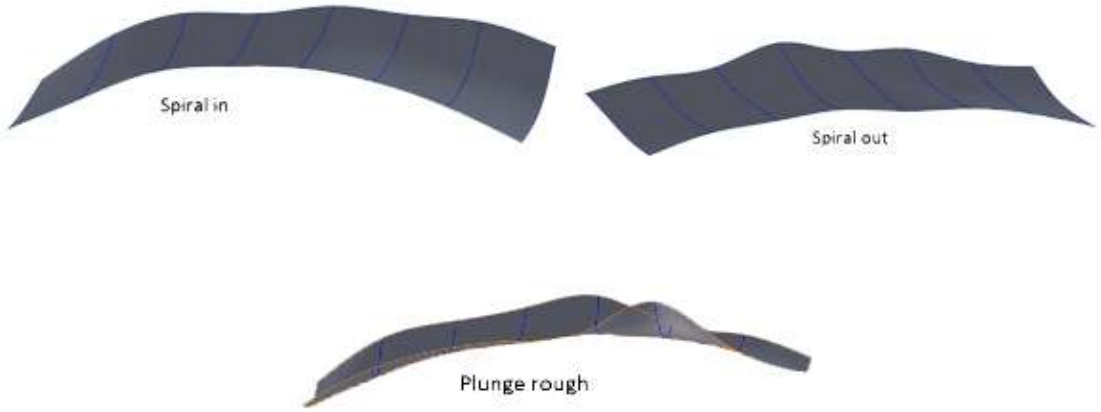

Figure 10:Profiles of the work pieces after machining in each toolpath layout

RESULTS AND DISCUSSION

The following inferences are drawn from data in Table 4 and its graphical representation in Figure 9.

1. The distribution of residual stress in X-axis in pocket in layout is tensile at the ends of the work piece where the tool starts machining. The residual stress changes from tensile to compressive and attains its peak value as the tool approaches the final stage of machining towards the centre. The residual stress in Y- axis is totally compressive having a magnitude relatively less compared to residual stress in X-axis.
2. The residual stress in X-axis in pocket out layout is tensile in most of the distribution profile, whereas residual stress in Y-axis is completely tensile.
3. The residual stresses in both X and Y axes in zig longitudinal layout are completely tensile.
4. The residual stress in zig transverse layout is compressive at the middle of the work piece and tensile in the remaining areas. The stress is distributed uniformly about the center. The residual stress in Y-axis is totally tensile.
5. The residual stresses in both X and Y axes inzig zag longitudinal layout are compressive at the middle of the work piece and tensile in the remaining areas. The stress in Y axis is distributed uniformly about the center.
6. The residual stress in Y axis in zig zag transverse layout is tensile in the initial stage of machining and gradually changed to compressive stress during the course of machining. It remained compressive till the final stage of machining. The magnitude of compressive stress is maximum at the centre.
7. The residual stress in spiral in layout in X axis changed from compressive to tensile in first half of machining and it changed from tensile to compressive during the second half of machining. The stress distribution trend in Y axis is same as in X axis.
8. The residual stress in spiral out layout in X axis is mostly compressive and in Y axis is totally compressive.
9. The residual stress in X axis in plunge rough layout is varying in both tensile and compressive ranges skewing towards compressive stress. The stress distribution pattern in Y axis is same as in X axis but totally compressive.
10. The maximum values of stress and stress ranges in X and Y axes are shown in Table 5.
11. From the measured values of deviations the distortion of work piece in different machining strategies in descending order is

    PLUNGE ROUGH> POCKET IN>ZIG ZAG LONGITUDINAL>ZIG LONGITUDINAL > SPIRAL IN > ZIG TRANSVERSE > ZIG ZAG TRANSVERSE > SPIRAL OUT > POCKET OUT and the maximum value of distortion is 0.803mm.
12. From the measured values of deviations the distortion range of work piece in different machining strategies in descending order is

    ZIG LONGITUDINAL > PLUNGE ROUGH > POCKET IN > ZIG ZAG LONGITUDINAL > ZIG TRANSVERSE >SPIRAL OUT > SPIRAL IN > ZIG ZAG TRANSVERSE > POCKET OUT

ISSN: 2277-9655
Impact Factor: 3.785

Table 5: STRESS RANGE VALUES IN DIFFERENT TOOLPATH LAYOUTS

TOOL PATH LAYOUT		Maximum STRESS IN X		Maximum STRESS IN Y		STRESS RANGE IN X	STRESS RANGE IN Y
SL.No		Tensile	Compressive	Tensile	Compressive		
1	POCKET IN	63.9	-56.4		-76.2	120.30	59.40
2	POCKET OUT	51.2	-8.8	54.0		60.00	51.50
3	ZIG LONGITUDINAL	31.6		108.1		25.90	107.65
4	ZIG TRANSVERSE	43.2	-26.2	65.0	-9.4	69.40	74.40
5	ZIG ZAG LONGITUDINAL	94	-24.4	68.7	-11.7	118.40	80.40
6	ZIG ZAG TRANSVERSE	48.8	-64.8	48.8	-59.9	113.60	108.70
7	SPIRAL IN	48.6	-30.3	26	-28.5	78.90	54.50
8	SPIRAL OUT	49.6	-133.3		-88.5	182.90	55.90
9	PLUNGE ROUGH	9.5	-98.7		-148.8	108.20	74.80

CONCLUSION

The measured values of distortion indicates that the work piece is twisted in all the X,Y and Z directions which is clearly evident from the stress values in Table 4, its graphical representation in Figure 9 and modeled profiles of the work piece after machining in Figure 10. The maximum distortion value and distortion range is lowest in pocket out layout and hence is widely preferred machining layout. The least preferred machining layout is plunge rough. The spiral out layout is also widely preferred in machining as induced compressive stress is maximum which is desirable for Avionic components for enhanced fatigue strength.

ACKNOWLEDGEMENT

The authors are thankful to the Head of Department,Osmania University for his constant encouragement and valuable guidance. The authors are alsothankful to the management of S.L.R.D.C(H.A.L) for permitting to conduct the experiments.

REFERENCES

[1] Totten, G. E., Scott Mackenzie D., Handbook of aluminum. New York, Marcel Dekker Inc.,2003
[2] Rowlands, R.E., 1987. Residual Stresses. In: Kobayashi, A. (Ed.), Handbook on Experimental Mechanics. Prentice-Hall, New Jersey, pp: 768-813.
[3] Lu, J., 1996. Handbook of Measurement of Residual Stresses. Fairmont Press Inc., Lilburn, Georgia.
[4] Withers, P.J. and H. Bhadeshia, 2001. Residual stress. Part 1 - measurement techniques. Mater. Sci. Technol., 17: 355-365.
[5] Fuh, K.H. and C. Wu, 1995. A residual stress model for the milling of aluminium alloy (2014-T6). J. Mater. Proc. Tech., 51: 87-105.
[6] M`Saoubi, R., J. Outeiro, J. Changeux, J. Lebrun and A. Morão Dias, 1999. Residual stress analysis in orthogonal machining of standard and resulfurized AISI 316 steels. J. Mater. Proc. Tech., 96: 225-233.
[7] M`Saoubi, R., J. Outeiro, J. Changeux, J. Lebrun and A. Morão Dias, 1999. Residual stress analysis in orthogonal machining of standard and resulfurized AISI 316 steels. J. Mater. Proc. Tech., 96: 225-233.
[8] Bouzid Saï, W., N. Ben Salah and J. Lebrun, 2001. Influence of machining by finishing milling on surface characteristics. Int. J. Mach. Tools Manufact., 4: 443-450.
[9] Wyatt, J.E. and J. Berry, 2006. A new technique for the determination of superficial residual stresses associated with machining and other manufacturing processes. J. Mater. Proc. Tech., 171: 132-140.
[10] Wei-Ming Sim1.Residual Stress Engineering in Manufacture of Aerospace Structural Parts
[11] H. C. Ye, G. H. Qin, C. K. Wang and D. Lu;A simulation study on the end milling operation with multiple process steps of aeronautical frame monolithic components

[12] Fuh, K.-H. and C.-F. Wu, Residual-Stress Model for the Milling of Aluminum Alloy (2014-T6). Journal of Materials Processing Technology, 1995. 51(1-4): p.87-105.
[13] BS EN 485-2:2013;Aluminium and aluminium alloys. Sheet, strip and plate. Mechanical properties
[14] F. V. Díaz, R. E. Bolmaro, A. P. M. Guidobono and E. F. Girini, "Determination of Residual Stresses in High Speed Milled Aluminium Alloys Using a Method of In-dent Pairs," Experimental Mechanics.
[15] C. A. Mammana, F. V. Díaz, A. P. M. Guidobono and R. Bolmaro, "Study of Residual Stress Tensors in High-Speed Milled Specimens of Aluminium Alloys Using a Method of Indent Pairs," Research Journal of Applied Sciences, Engineering and Technology, Vol. 2, No. 8, 2010, pp. 749-756.
[16] P. J. Withers and H. K. Bhadeshia, "Residual Stress. Part 1—Measurement Techniques," Materials Science and Technology.Vol. 17, No. 4, 2001, pp. 355-365.
[17] J. M. Gere, "Mechanics of Materials," Brooks/Cole, Pa-cific Grove, 2001
[18] F. V. Díaz, C. A. Mammana, A. P. M. Guidobono and R. E. Bolmaro, "Analysis of Residual Strain and
[19] StressDis-tributions in High Speed Milled Specimens Using an In- dentation Method," International Journal of Engineering and Applied Sciences, Vol. 7, No. 1, 2011, pp. 40-46.